Supplementary Material

Supplementary Methodology

Cardiovascular Risk Factors' Definitions

Cardiovascular risk factors (CVRFs), including age >65 years, male gender, glomerular filtration rate (GFR) below 60 mL/min/1.73 m^2, smoking, hypertension, hyperlipidemia, diabetes, obesity and increased high-sensitivity C-reactive protein (hs-CRP) (>2 mg/L)[1] were recorded for each participant and their sum was assessed as a measure of CVRF burden. Hypertension was defined as office blood pressure (BP) >140/90 mm Hg[2] or history of medical treatment with antihypertensive drugs. Diabetes mellitus (DM) was defined according to latest criteria as fasting plasma glucose ≥126 mg/dL[3] or intake of antidiabetic drugs. Hyperlipidemia was defined according to current guidelines by the lipid profile associated with the cardiovascular risk.[4] Smoking cessation was recorded as current or quitted >6 months. GFR was estimated by the Modification of Diet in Renal Disease equation.

Cardiovascular Risk Estimation

Patients were also classified into risk categories according to European Society of Cardiology (ESC) clinical criteria. In detail, ESC definition of very high risk patients includes the presence of any of the following: (1) documented cardiovascular disease (CVD), clinical or unequivocal on imaging. Documented clinical CVD includes previous acute myocardial infarction, acute coronary syndrome (ACS), coronary revascularization and other arterial revascularization procedures, stroke and transient ischemic attack, aortic aneurysm, and peripheral artery disease. Unequivocally documented CVD on imaging includes plaque on coronary angiography or carotid ultrasound. (2) DM with target organ damage such as proteinuria or with a major risk factor such as smoking or marked hypercholesterolemia or marked hypertension. (3) Severe chronic kidney disease (CKD; GFR < 30 mL/min/1.73 m^2). (4) A calculated SCORE ≥10%.[5]

ESC definition of high-risk patients includes the presence of any of the following: (1) Markedly elevated single risk factors, in particular cholesterol >8 mmol/L (>310 mg/dL) (e.g., in familial hypercholesterolemia) or BP ≥180/110 mm Hg; (2) most other people with DM (with the exception of young people with type 1 DM and without major risk factors that may be at low or moderate risk); (3) moderate CKD (GFR 30–59 mL/min/1.73 m^2); (4) a calculated SCORE ≥5% and <10%.[5]

Stable CAD and ACS Definition

Individuals were considered as stable CAD patients according to the following criteria: (1) patients who had undergone

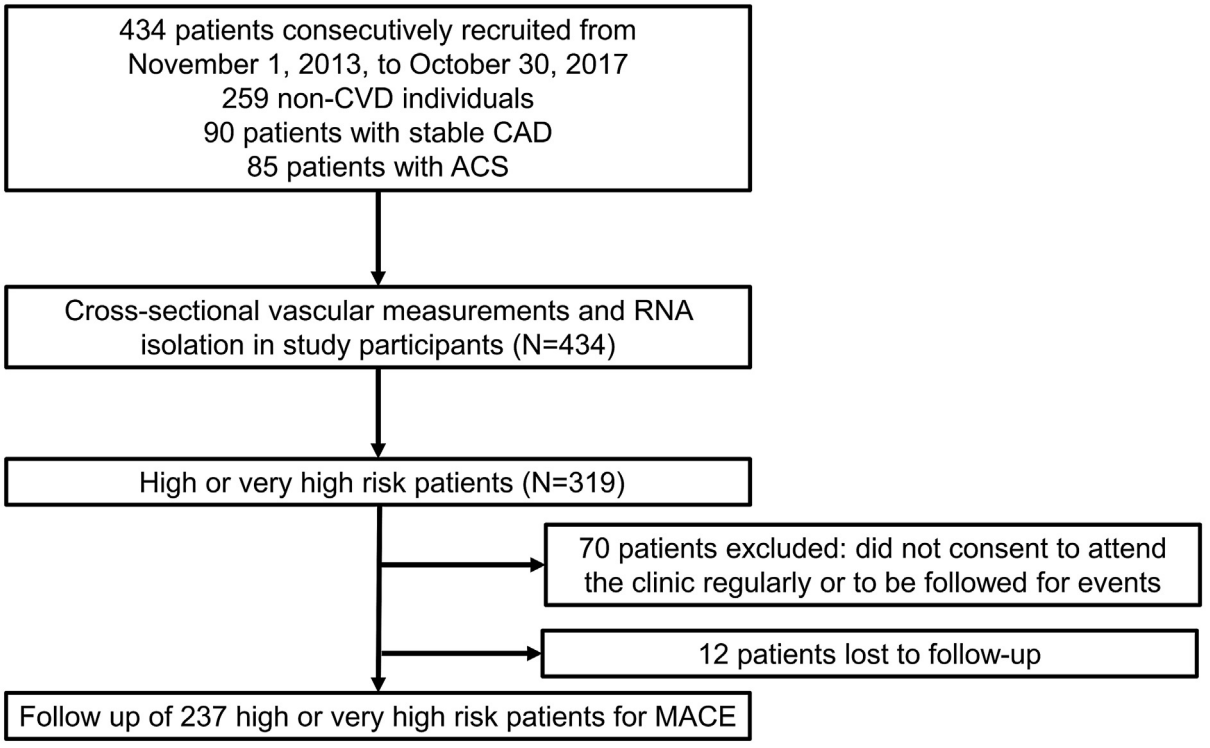

Supplementary Fig. S1 Flowchart of the study population. ACS, acute coronary syndrome; CVD, cardiovascular disease; CAD, coronary artery disease, MACE, major adverse cardiovascular events.

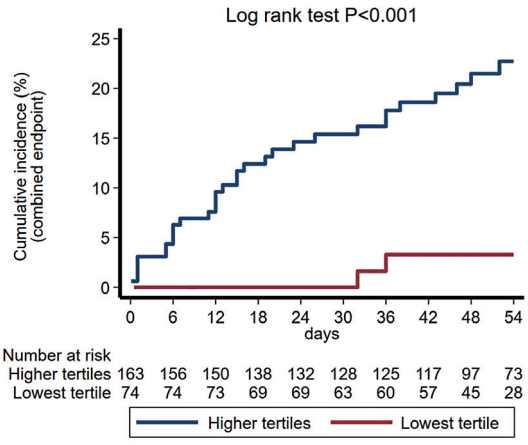

Supplementary Fig. S2 Cumulative incidence of major adverse cardiovascular events (cardiovascular death, acute myocardial infarction, and revascularization procedure) in high/very high CVD risk patients (total $N = 237$) according to *BACE1-AS* tertiles (lowest vs. higher), initially defined in the whole population. The number of patients at risk, during the follow-up period per *BACE1-AS* tertiles defined in the total population (lowest vs. higher), is depicted beneath the graph. $p < 0.001$ by log-rank test of equality. HR = 2.42 per ascending tertile (95% CI: 1.39–4.22), $p = 0.002$, by Cox regression analysis. HR = 1.86 per ascending tertile (95% CI: 1.011–3.43), $p = 0.046$, after multivariable adjustment for age, gender, presence of coronary artery disease, diabetes mellitus, and hypertension. CI, confidence interval; CVD, cardiovascular disease; HR, hazard ratio.

an elective coronary angiogram within the previous month, due to stable angina symptoms or chest pain not attributed to ACS or aortic syndrome, (2) previous history of ACS more than a year before baseline visit, and (3) documented presence of CAD by coronary angiogram or by stress imaging techniques.[6] A diseased coronary artery was defined as >50% stenosis.[6] ACS was defined as increased high sensitivity cardiac troponin levels (>99th percentile) combined with at least one of the following: (1) symptoms of ischemia, (2) ECG abnormalities, i.e., ST-T segment alterations, left bundle branch block, or Q waves, (3) imaging evidence of new loss of viable myocardium or regional wall motion abnormality, and (4) intracoronary thrombus detected with coronary angiography or autopsy.[7]

Vascular Methods

Peripheral vascular assessment was performed in all participants without clinically overt CVD and in patients with CAD (stable CAD or ACS). Aortic stiffness was assessed by aortic pulse wave velocity (PWV), an established marker of aortic elasticity.[8–10] The validated Complior device (Artech Medical), which allows the online pulse-wave recording and the automatic calculation of PWV, was used to assess PWV noninvasively. PWV values were derived from measurements of pulse transit time and the distance travelled

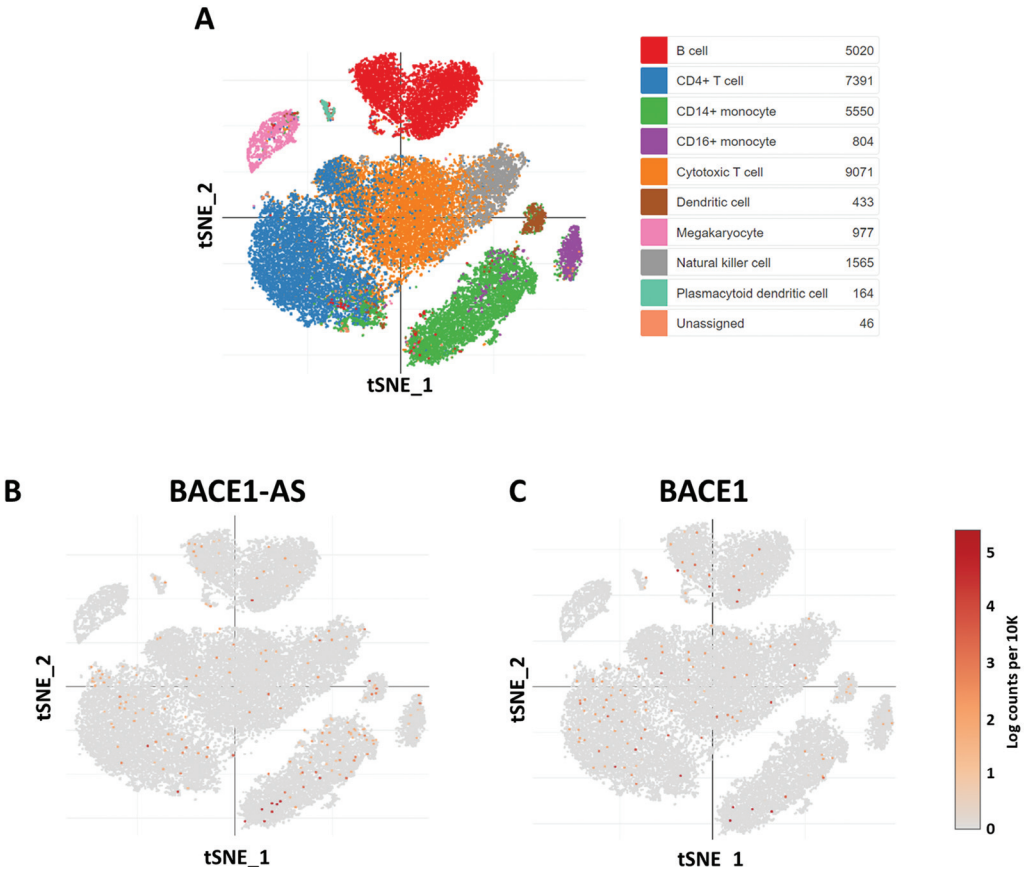

Supplementary Fig. S3 t-Distributed stochastic neighbor embedding (tSNE) projections of *BACE1-AS* and *BACE1* gene expression in human PBMCs. (**A**) t-SNE plot of colored and labeled cell clusters showing their respective cell subtypes across PBMCs. (**B, C**) The gene expression of *BACE1-AS* and *BACE1* in PBMC subtypes. Each dot represents a single cell. Dots colored in *red* indicate the gene expression of which the warmer the color the higher the fold change in gene expression. PBMCs, peripheral blood mononuclear cells.

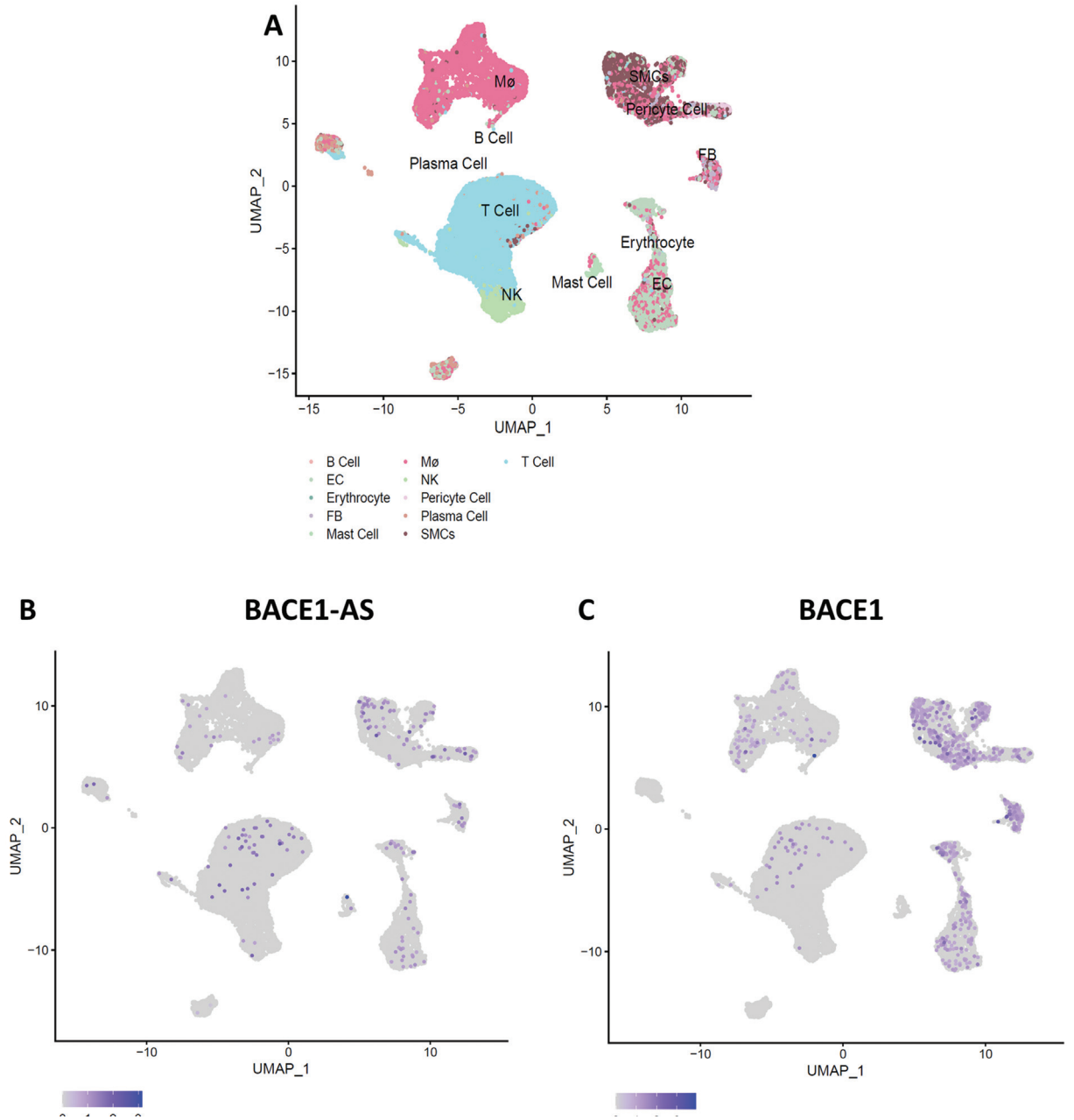

Supplementary Fig. S4 Single-cell analysis results of *BACE1-AS* and *BACE1* gene expression in human atherosclerotic plaque. (**A**) UMAP plot of the proportion of diverse cell subtypes across atherosclerotic plaque with labels based on Seurat v4 using the Tabula sapiens reference. (**B, C**) UMAP plot showing the distribution of *BACE1-AS* and *BACE1* in atherosclerotic plaque different cell subtypes. Dot size depicts the fraction of cells expressing a gene. Dot color depicts the degree of expression of each gene. UMAP, uniform manifold approximation and projection for dimension reduction.

between two recording sites, and automatically calculated as follows: PWV = distance [m]/transit time [s]. In our study, PWV was measured between the common carotid artery and the common femoral artery and assessed twice (coefficient of variation: 2.4%). Reference values for PWV were used according to each subject's systolic BP and age, as previously described.[11]

High-resolution B-mode ultrasound imaging (14.0 MHz multifrequency linear array probe, Vivid 7 Pro, General Electric) was used to assess carotid and common femoral artery atherosclerosis and to measure intima-media thickness (IMT) and atheromatous plaques.[12] IMT was measured between the intimal luminal and the medial adventitial interfaces of the carotid and femoral far wall, at the end-diastolic phase.[13] Atheromatous plaques were defined as a focal thickening that encroaches into the arterial lumen by 0.5 mm, or by 50% of the surrounding IMT, or sites where IMT is >1.5 mm.[12] All scans were performed by a single experienced operator blinded to the cardiovascular profile of the patient.

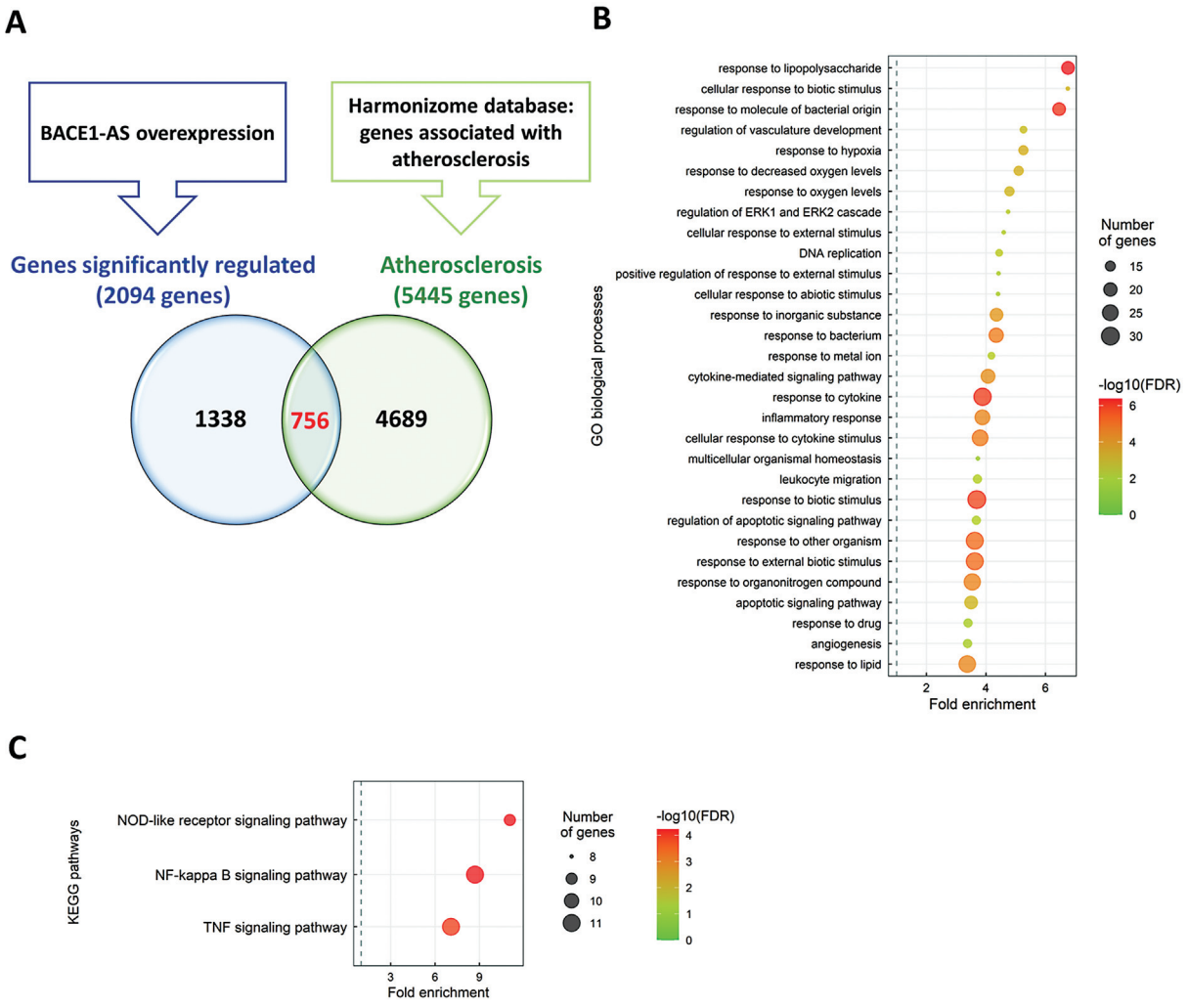

Supplementary Fig. S5 Pipeline used to identify validated targets of *BACE1-AS* involved in atherosclerosis. (**A**) We identified 2,094 genes significantly regulated with a corrected *p*-value of <0.05 after *BACE1-AS* overexpression in human aortic endothelial cells, from which 756 are predicted to be involved in atherosclerosis according to the Harmonizome database (https://maayanlab.cloud/Harmonizome/). (**B**) Gene ontology analysis of the 756 atherosclerotic genes regulated by *BACE1-AS* overexpression (provided as input), using the web-based tool and applying the following criteria: GOTERM_BP_FAT as selected terms and displayed terms with >10 counts in a functional annotation chart. (**C**) KEGG pathway enrichment analysis to explore the most enriched pathways among the 756 atherosclerotic genes regulated by *BACE1-AS* overexpression. The output pathways were filtered for false discovery rate (FDR) <0.05 and fold enrichment >1.5. Subsequently, the pathways were sorted for increasing fold enrichment and plotted. In the plot, the size of each dot represents the number of genes from the input gene set included in each pathway while the color indicates the FDR value (as $-\log10(\text{FDR})$).

Supplementary Table S1 Descriptive characteristics of high/very high CVD risk patients ($N = 237$) who were followed for events compared with high/very high-risk; CVD patients lost during follow-up ($N = 12$)

Variable	*N*	All	Followed ($N = 237$)	Lost to follow-up ($N = 12$)	*p*-Value
Age (y)	249	61.59 (10.03)	61.56 (10.13)	62.08 (8.16)	0.835
Gender (male), *n* (%)	239	155 (64.85%)	146 (61.6%)	7 (58.3%)	0.803
Non-CVD, *n* (%)	134		128 (54%)	6 (50%)	0.686
Stable CAD, *n* (%)	56		54 (22.8%)	2 (16.6%)	0.699
ACS, *n* (%)	59		55 (23.2%)	4 (33.3%)	0.686
BACE1-AS relative expression	249	0.00613 (0.0052)	0.0061 (0.0052)	0.0071 (0.0057)	0.575
BMI (kg/m^2)	206	27.60 (4.34)	27.63 (4.34)	26.80 (3.67)	0.585
SBP (mmHg)	210	132.60 (20.109)	132.60 (20.34)	132.60 (15.53)	0.999
DBP (mmHg)	210	75.13 (10.68)	75.12 (10.50)	75.40 (14.50)	0.952
Smoking, *n* (%)	248	109 (43.6%)	104 (43.5%)	5 (41.66%)	0.870
Hypertension, *n* (%)	249	122 (48.8%)	116 (48.9%)	6 (50%)	0.921
Hyperlipidemia, *n* (%)	249	132 (52.8%)	126 (53.2%)	6 (50%)	0.090
Diabetes mellitus, *n* (%)	249	43 (19.4%)	40 (16.9%)	3 (25%)	0.458
Presence of carotid plaques, *n* (%)	222	141 (54.9%)	132 (55.7%)	8 (66.67%)	0.268
Presence of any plaque, *n* (%)	220	167 (63.3%)	160 (67.5%)	7 (58.33%)	0.919
Presence of femoral plaques, *n* (%)	221	122 (47.3%)	115 (48.5%)	6 (50%)	0.528
*GFR (mL/min)	30	88.53 (34.23)	87.32 (33.20)	113.06 (45.18)	0.076
*hs-CRP (mg/L)	229	2.52 (11.94)	2.50 (12.16)	2.95 (4.40)	0.784
*Pulse wave velocity (m/s)	177	10.15 (2.91)	10.13 (2.89)	10.58 (3.48)	0.731
*Augmentation index (%)	166	27.61 (21.99)	27.51 (22.45)	29.75 (9.31)	0.561
*Time of reflected waves (ms)	168	138.5 (11.03)	138.96 (9.82)	127.50 (16.66)	0.094
* Common carotid artery IMT (mm)	207	0.894 (0.173)	0.89 1(0.172)	0.974 (0.183)	0.214
*Carotid bulb IMT (mm)	184	1.026 (0.191)	1.027 (0.193)	1.01 (0.187)	0.872
*Internal carotid IMT (mm)	187	0.843 (0.228)	0.844 (0.226)	0.817 (0.302)	0.810
*Number of carotid plaques (IQR)	227	1 (0–2)	1 (0–2)	1 (0–2)	0.884
*Total number of femoral and carotid segments with plaque (IQR)	226	1 (0–3)	1(0–3)	3 (1–5)	0.863
*Number of diseased vascular beds (IQR)	249	1 (1–3)	1 (1–3)	1(1–3)	0.689

Abbreviations: ACS, acute coronary syndrome; BMI, body mass index; CAD, coronary artery disease; hs-CRP, high-sensitivity C-reactive protein; CVD, cardiovascular disease; DBP, diastolic blood pressure; GFR, glomerular filtration rate; IMT, intima-media thickness; IQR, interquartile range; SBP, systolic blood pressure.

Note: Diseased vascular beds were defined as: (1) carotid arteries with presence of plaque, (2) coronary arteries with presence of plaque with stenosis >50%, (3) femoral arteries with presence of plaque. *p*-Value is derived from independent samples; Student's *t*-test or the non-parametric Mann–Whitney U test (*) for continuous variables and the chi-squared test for nominal variables.

Supplementary Table S2 Descriptive characteristics of high/very high CVD risk patients ($N = 237$) who were followed for events according to *BACE1-AS* tertiles

Variable	*N*	All	1st tertile	2nd tertile	3rd tertile	*p*-Value
Age (y)	236	61.6 (11.2)	59.4(9.9)	64 (10.9)	61.3 (9.1)	0.012
Gender (male), *n* (%)	237	146 (61.6%)	47 (59.5)	47 (59.5%)	52 (65.8%)	0.640
Non-CVD, *n* (%)	128	128 (54%)	59 (74.7%)	34 (43%)	35 (44.3%)	<0.001
Stable CAD, *n* (%)	54	54 (22.8%)	9 (11.4%)	26 (32.9%)	19 (24.1%)	<0.001
ACS, *n* (%)	55	55 (23.2%)	11 (13.9%)	19 (24.1%)	25 (31.6%)	<0.001
BMI (kg/m^2)	195	27.66 (4.36)	28.15 (4.62)	27.14 (4.01)	27.56 (4.34)	0.495
SBP (mmHg)	198	132.58 (20.28)	134.36 (19.89)	130.25 (20.6)	132.81 (20.86)	0.563
DBP (mmHg)	198	75.08 (10.46)	74.99 (10.40)	74.05 (9.77)	76.07 (11.16)	0.598
Smoking, *n* (%)	234	103 (44%)	29 (36.7%)	31 (40.3%)	43 (55.1%)	0.048
Hypertension, *n* (%)	237	116 (48.9%)	31(39.2%)	46 (58.2%)	39 (49.4%)	0.058
Hyperlipidemia (%)	237	126 (53.2%)	32 (40.5%)	46 (58.2%)	48 (60.8%)	0.039
Diabetes mellitus, *n* (%)	237	40 (16.9%)	11 (27.5%)	15 (19%)	14 (17.7%)	0.676
Presence of carotid plaques, *n* (%)	210	132 (62.9%)	46 (64.8%)	42 (57.5%)	44 (66.7%)	0.494
Presence of any plaque, *n* (%)	209	212 (56.68%)	56 (78.9%)	54 (74.0%)	50 (76.9%)	0.783
Presence of femoral plaques (%)	209	115 (55%)	38 (53.5%)	37 (51.4%)	40 (60.6%)	0.527
*GFR (mL/min)	230	87.28 (33.34)	94.83 (33.19)	78.99 (32.29)	85.80 (32.97)	0.008
*hs-CRP (mg/L)	217	0.23 (0.08–0.875)	3.26 (18.95)	1.61 (4.80)	2.67 (8.35)	0.110
*Pulse wave velocity (m/s)	167	10.12 (2.88)	9.51 (2.49)	10.46 (2.90)	10.49 (3.19)	0.086
*Augmentation index (%)	156	27.58 (22.57)	25.17 (8.02)	32.48 (41.34)	26.42 (8.12)	0.694
*Time of return of reflected waves (ms)	158	140 (133–146)	141.54 (8.72)	138.26 (9.61)	136.38 (10.35)	0.011
*Common carotid artery IMT (mm)	196	0.89 (0.172)	0.87(0.18)	0.89 (0.17)	0.91 (0.17)	0.480
*Total number of femoral and carotid segments with plaque	214	1 (0–2)	0 (0–2)	1 (0–3)	1 (0–3)	0.770
*Number of diseased vascular beds	237	1 (0–2)	1 (0–2)	1 (1–3)	1 (1–3)	0.732

Abbreviations: BMI, body mass index; hs-CRP, high-sensitivity C-reactive protein; DBP, diastolic blood pressure; GFR, glomerular filtration rate; IMT, intima-media thickness; SBP, systolic blood pressure.
Note: *p*-Value is derived from analysis of variance or the nonparametric Kruskal–Wallis rank test (*) for continuous variables and the chi-squared test for nominal variables. Diseased vascular beds were defined as: (1) carotid arteries with presence of plaque, (2) coronary arteries with presence of plaque with stenosis >50%, (3) femoral arteries with presence of plaque.

Supplementary Table S3 Literature curation regarding the proatherosclerotic role of *BACE1* and *BACE1-AS*

Experimental model	Study finding	Source
BACE1 repression		
***BACE1*$^{-/-}$ mice fed with high-fat diet**	Lower levels of circulating LDL and TGs Reduction of atherosclerotic plaque	[14]
***BACE1*$^{-/-}$ macrophages**	Decrease number of lipid droplets in the foam cells	[14]
***BACE1*$^{-/-}$ mice (serum)**	Increase anti-inflammatory IL-9 production	[15]
Human monocyte cell line treated with *BACE1* inhibitor	Reduce binding to VCAM-1 *BACE1* is markedly upregulated during macrophage differentiation	[16]
***BACE1*$^{-/-}$ mice**	Reduced IL-17A expression in *BACE1*$^{-/-}$ T cells	[17]
BACE1 overexpression		
Endothelial-specific *BACE1* overexpression mice	Tight junction disruptions and endothelial dysfunction	[18]
EA.hy926 endothelial cells treated with *BACE1*-overexpressing lentivirus	Increased endothelial cell tight junction disruption Increased monocyte adhesion	[19]
***BACE1-AS* repression**		
SH-SY5Y cells treated with *BACE1-AS* siRNA	Reduction of TNF-α, IL-6, IL-1β levels, and ROS production	[20]

Abbreviations: *BACE1,* beta-secretase-1; IL, interleukin; KO, knockout; LDL, low-density lipoprotein; NFκB, nuclear factor kappa B; TGs, triglycerides; TNF, tumor necrosis factor; TNFR1, tumor necrosis factor receptor-1.

Supplementary Table S4 Experimental and clinical data suggesting the involvement of *BACE1-AS* in the pathophysiology of multiple human diseases

Involvement of *BACE1-AS* in human disease						
Disease	**Target pathway**	**Function of pathway**	**Clinical relevance**	**Setting of association (animal experiment, cells, patients)**	**Effect of *BACE1-AS* on the target**	**References**
Alzheimer's disease	miR-29, miR-107, miR-124, miR-485 miR-761/*BACE* mRNA axis	miRNAs bind to *BACE* mRNA and suppress its translation		SH-SY5Y cell HEK293 T cells PP/PS1 transgenic mice	*BACE1-AS* sponges miR-124 miR-29, miR-107, miR-124, miR-485 miR-761	21
Alzheimer's disease	miR-214–3-p/ATG5 axis in AD.	miR-214–3p/ATG5 axis regulates neuronal cell autophagy	Elevated circulating *BACE1-AS* could serve as a biomarker	Serum samples of AD patients, brain tissues of AD transgenic (Tg) mice and SH-SY5Y cells	*BACE1-AS* sponges miR-214–3p and promotes autophagy in vivo.	22,23
Alzheimer's disease	miR-132–3p	Mitigates amyloid-induced neuronal toxicity		HEK293T cells SK-N-SH cells	*BACE1-AS* increased the amyloid-induced damage by sponging miR-132–3p	24
Parkinson's disease	miR34-b	miR34-b binds *BACE1* mRNA and decreases *BACE-1* expression		Substantia nigra tissue from Parkinson's disease mouse model	*BACE1-AS* sequesters miR34-b *BACE1-AS* promotes *BACE*1 expression by directly stabilizing *BACE1* mRNA and, indirectly, by sequestering miR34-B	25
Ovarian cancer	Unknown	Anisomycin treatment increases *BACE1-AS* and *BACE1*	Amyloid-induced cytotoxicity within the tumor	Human ovarian cancer stem cells	*BACE1-AS* stabilizes *BACE1* mRNA and thus promotes amyloid formation	26
Hepatocellular carcinoma (HCC)	miR-377–3-p/CELF1 axis	MiR-377–3p inhibits HCC cell migration and invasion. CELF1 is an oncogene in HCC cells and is downregulated by miR-377–3p.	*BACE1-AS* could be a potential biomarker in HCC	HCC tumor tissues and cells	*BACE1-AS* downregulates miR-377–3p and promotes tumor invasion and metastasis.	27,28
Sporadic inclusion-body myositis	Unknown	*BACE1-AS* increases in response to endoplasmic reticulum stress		Muscle tissue biopsy	*BACE1-AS* promotes Aβ formation in muscle tissue	29
Chronic inflammatory demyelinating polyradiculoneuropathy		Possible role of *BACE1*/*BACE1-AS* in immune response	*BACE1-AS* could serve as a biomarker	Peripheral blood		30

Abbreviations: *BACE1-AS,* β-secretase 1 anti-sense RNA; miR, microRNA; HAND, HIV-associated neurocognitive disorder; mRNA, messenger RNA.

Supplementary Table S5 Cardioprotective role of miRNAs sponged by *BACE1-AS*

microRNA	Methodology	Association with CVD
miR29	ACS, atrial fibrillation, and heart failure patients.	Downregulated in ACS, Afib, and HF patients.[31–33]
miR34b	VSMCs of spontaneously hypertensive rats, VSMCs from C57/BL mice.	Regulates VSMC proliferation by suppressing CDK6. miR-34b modulates VSMC calcification by directly targeting Notch1.[34,35]
miR107	Vascular endothelial cells of SPF Kunming mice, blood cells from patients with atherosclerosis.	Upregulation of miR-107 protects against inflammation in coronary atherosclerosis. Downregulated in patients with atherosclerosis, inhibits proliferation of HUVECs and HUVSMCs.[36,37]
miR124	CAD patients, PAD patients, ApoE$^{-/-}$, C57B/L6J mice, macrophages from ApoE$^{-/-}$ mice.	Downregulated in CAD patients, negatively associated with severity of PAD. miR-124 inhibits inflammatory responses during atherosclerosis development. Suppresses p38MAPK signaling pathway, inhibiting macrophage proliferation.[38–41]
miR132		Conflicting data.[41–48]
miR214	CAD patients, in vitro myocardial cells.	Decreased in CAD, UA, and AMI patients. Exerts cardioprotective properties in MI-induced cardiac injury.[49,50]
miR377	Human VSMCs.	Inhibits VSMC proliferation.[51]
miR485	CAD patients, in vitro myocardial cells.	Increased circulating miR485 in CAD patients. Inhibits cell autophagy and apoptosis of myocardial cells in vitro.[52,53]
miR761	Macrophages incubated with ox-LDL, rat aortic VSMCs.	Reduces IL-1β and IL-18 secretion in macrophages. miR-761 suppresses Ang-II-induced cell cycle progression and subsequent proliferation of VSMCs by inhibiting mTOR signaling pathway.[54,55]

Abbreviations: ACS, acute coronary syndrome; Afib, atrial fibrillation; AMI, acute myocardial infarction; AngII, angiotensin-II; ApoE, apolipoprotein-E; *BACE1-AS,* β-secretase 1 antisense RNA; CAD, coronary artery disease; CDK6, cycline-dependent kinase-6; CVD, cardiovascular disease; HF, heart failure; HUVECs, human umbilical vein endothelial cells; HUVSMCs, human umbilical vein smooth muscle cells; IL, interleukin; miR, microRNA; ox-LDL, oxidized low-density lipoprotein; PAD, peripheral artery disease; UA, unstable angina; VSMCs, vascular smooth muscle cells.

Conflict of Interest

The authors declare that there is no conflict of interest.

References

1 Yousuf O, Mohanty BD, Martin SS, et al. High-sensitivity C-reactive protein and cardiovascular disease: a resolute belief or an elusive link? J Am Coll Cardiol 2013;62(05):397–408

2 Williams B, Mancia G, Spiering W, et al; ESC Scientific Document Group. 2018 ESC/ESH guidelines for the management of arterial hypertension. Eur Heart J 2018;39(33):3021–3104

3 American Diabetes Association. 2. Classification and diagnosis of diabetes: *Standards of Medical Care in Diabetes-2020*. Diabetes Care 2020;43(Suppl 1):S14–S31

4 Mach F, Baigent C, Catapano AL, et al; ESC Scientific Document Group. 2019 ESC/EAS guidelines for the management of dyslipidaemias: lipid modification to reduce cardiovascular risk. Eur Heart J 2020;41(01):111–188

5 Piepoli MF, Hoes AW, Agewall S, et al; ESC Scientific Document Group. 2016 European guidelines on cardiovascular disease prevention in clinical practice: The Sixth Joint Task Force of the European Society of Cardiology and Other Societies on Cardiovascular Disease Prevention in Clinical Practice (constituted by representatives of 10 societies and by invited experts)Developed with the special contribution of the European Association for Cardiovascular Prevention & Rehabilitation (EACPR). Eur Heart J 2016;37(29):2315–2381

6 Knuuti J, Wijns W, Saraste A, et al; ESC Scientific Document Group. 2019 ESC guidelines for the diagnosis and management of chronic coronary syndromes. Eur Heart J 2020;41(03):407–477

7 Thygesen K, Alpert JS, Jaffe AS, et al; Executive Group on behalf of the Joint European Society of Cardiology (ESC)/American College of Cardiology (ACC)/American Heart Association (AHA)/World Heart Federation (WHF) Task Force for the Universal Definition of Myocardial Infarction. Fourth universal definition of myocardial infarction (2018). J Am Coll Cardiol 2018;72(18):2231–2264

8 Williams B, Lacy PS, Thom SM, et al; CAFE Investigators Anglo-Scandinavian Cardiac Outcomes Trial Investigators CAFE Steering Committee and Writing Committee. Differential impact of blood pressure-lowering drugs on central aortic pressure and clinical outcomes: principal results of the Conduit Artery Function Evaluation (CAFE) study. Circulation 2006;113(09):1213–1225

9 Niiranen TJ, Kalesan B, Larson MG, et al. Aortic-brachial arterial stiffness gradient and cardiovascular risk in the community: the Framingham Heart Study. Hypertension 2017;69(06):1022–1028

10 Cohn JN, Quyyumi AA, Hollenberg NK, Jamerson KA. Surrogate markers for cardiovascular disease: functional markers. Circulation 2004;109(25, Suppl 1):IV31–IV46

11 Townsend RR, Wilkinson IB, Schiffrin EL, et al; American Heart Association Council on Hypertension. Recommendations for improving and standardizing vascular research on arterial stiffness: a scientific statement from the American Heart Association. Hypertension 2015;66(03):698–722

12 Touboul PJ, Hennerici MG, Meairs S, et al. Mannheim carotid intima-media thickness and plaque consensus (2004-2006-

2011). An update on behalf of the advisory board of the 3rd, 4th and 5th watching the risk symposia, at the 13th, 15th and 20th European Stroke Conferences, Mannheim, Germany, 2004, Brussels, Belgium, 2006, and Hamburg, Germany, 2011. Cerebrovasc Dis 2012;34(04):290–296
13 Nambi V, Chambless L, Folsom AR, et al. Carotid intima-media thickness and presence or absence of plaque improves prediction of coronary heart disease risk: the ARIC (Atherosclerosis Risk In Communities) study. J Am Coll Cardiol 2010;55(15):1600–1607
14 Chen L, Huang Y, Guo J, Li Y. Expression of Bace1 is positive with the progress of atherosclerosis and formation of foam cell. Biochem Biophys Res Commun 2020;528(03):440–446
15 Stertz L, Contreras-Shannon V, Monroy-Jaramillo N, Sun J, Walss-Bass C. BACE1-deficient mice exhibit alterations in immune system pathways. Mol Neurobiol 2018;55(01):709–717
16 Woodard-Grice AV, McBrayer AC, Wakefield JK, Zhuo Y, Bellis SL. Proteolytic shedding of ST6Gal-I by BACE1 regulates the glycosylation and function of alpha4beta1 integrins. J Biol Chem 2008;283 (39):26364–26373
17 Hernandez-Mir G, Raphael I, Revu S, et al. The Alzheimer's disease-associated protein BACE1 modulates T cell activation and Th17 function. J Immunol 2019;203(03):665–675
18 Zhou H, Gao F, Yang X, et al. Endothelial BACE1 impairs cerebral small vessels via tight junctions and eNOS. Circ Res 2022;130(09): 1321–1341
19 Deng X, Zhang J, Liu Y, Chen L, Yu C. TNF-α regulates the proteolytic degradation of ST6Gal-1 and endothelial cell-cell junctions through upregulating expression of BACE1. Sci Rep 2017;7:40256
20 Li L, Wang H, Li H, Lu X, Gao Y, Guo X. Long noncoding RNA BACE1-antisense transcript plays a critical role in Parkinson's disease via microRNA-214-3p/Cell death-inducing p53-target protein 1 axis. Bioengineered 2022;13(04):10889–10901
21 Zeng T, Ni H, Yu Y, et al. BACE1-AS prevents BACE1 mRNA degradation through the sequestration of BACE1-targeting miRNAs. J Chem Neuroanat 2019;98:87–96
22 Zhou Y, Ge Y, Liu Q, et al. LncRNA BACE1-AS promotes autophagy-mediated neuronal damage through the miR-214-3p/ATG5 signalling axis in Alzheimer's disease. Neuroscience 2021; 455:52–64
23 Wang J, Wang WN, Xu SB, et al. MicroRNA-214-3p: a link between autophagy and endothelial cell dysfunction in atherosclerosis. Acta Physiol (Oxf) 2018;222(03):
24 Ge Y, Song X, Liu J, Liu C, Xu C. The combined therapy of berberine treatment with lncRNA BACE1-AS depletion attenuates $A\beta_{25-35}$ induced neuronal injury through regulating the expression of miR-132-3p in neuronal cells. Neurochem Res 2020;45(04): 741–751
25 Li Y, Fang J, Zhou Z, et al. Downregulation of lncRNA BACE1-AS improves dopamine-dependent oxidative stress in rats with Parkinson's disease by upregulating microRNA-34b-5p and downregulating BACE1. Cell Cycle 2020;19(10):1158–1171
26 Chen Q, Liu X, Xu L, et al. Long non-coding RNA BACE1-AS is a novel target for anisomycin-mediated suppression of ovarian cancer stem cell proliferation and invasion. Oncol Rep 2016;35 (04):1916–1924
27 Liu C, Wang H, Tang L, et al. LncRNA BACE1-AS enhances the invasive and metastatic capacity of hepatocellular carcinoma cells through mediating miR-377-3p/CELF1 axis. Life Sci 2021; 275:119288
28 Nie Y, Li Y, Xu Y, Jiao Y, Li W. Long non-coding RNA BACE1-AS is an independent unfavorable prognostic factor in liver cancer. Oncol Lett 2020;20(05):202
29 Nogalska A, Engel WK, Askanas V. Increased BACE1 mRNA and noncoding BACE1-antisense transcript in sporadic inclusion-body myositis muscle fibers–possibly caused by endoplasmic reticulum stress. Neurosci Lett 2010;474(03):140–143
30 Ghafouri-Fard S, Mazdeh M, Nicknafs F, Nazer N, Sayad A, Taheri M. Expression analysis of BDNF, BACE1 and their antisense transcripts in inflammatory demyelinating polyradiculoneuropathy. Mult Scler Relat Disord 2021;47:102613
31 Dawson K, Wakili R, Ordög B, et al. MicroRNA29: a mechanistic contributor and potential biomarker in atrial fibrillation. Circulation 2013;127(14):1466–1475, 1475e1–28
32 Leptidis S, El Azzouzi H, Lok SI, et al. A deep sequencing approach to uncover the miRNOME in the human heart. PLoS One 2013;8 (02):e57800
33 Shen L, Song Y, Fu Y, Li P. MiR-29b mimics promotes cell apoptosis of smooth muscle cells via targeting on MMP-2. Cytotechnology 2018;70(01):351–359
34 Yang F, Li H, Du Y, Shi Q, Zhao L. Downregulation of microRNA–34b is responsible for the elevation of blood pressure in spontaneously hypertensive rats. Mol Med Rep 2017;15(03):1031–1036
35 Lin X, Li F, Xu F, et al. Aberration methylation of miR-34b was involved in regulating vascular calcification by targeting Notch1. Aging (Albany NY) 2019;11(10):3182–3197
36 Gao ZF, Ji XL, Gu J, Wang XY, Ding L, Zhang H. microRNA-107 protects against inflammation and endoplasmic reticulum stress of vascular endothelial cells via KRT1-dependent Notch signaling pathway in a mouse model of coronary atherosclerosis. J Cell Physiol 2019;234(07):12029–12041
37 Shen L, Hu Y, Lou J, et al. CircRNA–0044073 is upregulated in atherosclerosis and increases the proliferation and invasion of cells by targeting miR–107. Mol Med Rep 2019;19(05):3923–3932
38 Liang X, Wang L, Wang M, et al. MicroRNA-124 inhibits macrophage cell apoptosis via targeting p38/MAPK signaling pathway in atherosclerosis development. Aging (Albany NY) 2020;12(13): 13005–13022
39 de Ronde MWJ, Kok MGM, Moerland PD, et al. High miR-124-3p expression identifies smoking individuals susceptible to atherosclerosis. Atherosclerosis 2017;263:377–384
40 Shi Y, Xu X, Luan P, et al. miR–124–3p regulates angiogenesis in peripheral arterial disease by targeting STAT3. Mol Med Rep 2020;22(06):4890–4898
41 Zhai C, Cong H, Hou K, et al. Effects of miR-124-3p regulation of the p38MAPK signaling pathway via MEKK3 on apoptosis and proliferation of macrophages in mice with coronary atherosclerosis. Adv Clin Exp Med 2020;29(07):803–812
42 Choe N, Kwon JS, Kim JR, et al. The microRNA miR-132 targets Lrrfip1 to block vascular smooth muscle cell proliferation and neointimal hyperplasia. Atherosclerosis 2013;229(02):348–355
43 Zhang L, Huang D, Wang Q, et al. MiR-132 inhibits expression of SIRT1 and induces pro-inflammatory processes of vascular endothelial inflammation through blockade of the SREBP-1c metabolic pathway. Cardiovasc Drugs Ther 2014;28(04):303–311
44 Fu C, Yin D, Nie H, Sun D. Notoginsenoside R1 protects HUVEC against oxidized low density lipoprotein (Ox-LDL)-induced atherogenic response via down-regulating miR-132. Cell Physiol Biochem 2018;51(04):1739–1750
45 Chen WJ, Chen YH, Hsu YJ, Lin KH, Yeh YH. MicroRNA-132 targeting PTEN contributes to cilostazol-promoted vascular smooth muscle cell differentiation. Atherosclerosis 2018;274:1–7
46 Niespolo C, Johnston JM, Deshmukh SR, et al. Tribbles-1 expression and its function to control inflammatory cytokines, including interleukin-8 levels are regulated by miRNAs in macrophages and prostate cancer cells. Front Immunol 2020;11:574046
47 Šatrauskienė A, Navickas R, Laucevičius A, et al. Mir-1, miR-122, miR-132, and miR-133 are related to subclinical aortic atherosclerosis associated with metabolic syndrome. Int J Environ Res Public Health 2021;18(04):1483

48 Wang W, Li X, Ren L, Yuan C, Han Y, Wang Z. MiR-132 relieves vascular endothelial inflammation and improves endothelial function in atherosclerosis rats by regulating SIRT1. Minerva Endocrinol 2020;45(02):158–161
49 Zhao Y, Ponnusamy M, Zhang L, et al. The role of miR-214 in cardiovascular diseases. Eur J Pharmacol 2017;816:138–145
50 Lu HQ, Liang C, He ZQ, Fan M, Wu ZG. Circulating miR-214 is associated with the severity of coronary artery disease. J Geriatr Cardiol 2013;10(01):34–38
51 Wang H, Wei Z, Li H, et al. MiR-377-3p inhibits atherosclerosis-associated vascular smooth muscle cell proliferation and migration via targeting neuropilin2. Biosci Rep 2020;40(06):BSR20193425
52 Zhou J, Li L, Hu H, et al. Circ-HIPK2 accelerates cell apoptosis and autophagy in myocardial oxidative injury by sponging miR-485-5p and targeting ATG101. J Cardiovasc Pharmacol 2020;76(04):427–436
53 D'Alessandra Y, Carena MC, Spazzafumo L, et al. Diagnostic potential of plasmatic MicroRNA signatures in stable and unstable angina. PLoS One 2013;8(11):e80345
54 Wang C, Yang W, Liang X, et al. MicroRNA-761 modulates foam cell formation and inflammation through autophagy in the progression of atherosclerosis. Mol Cell Biochem 2020;474(1-2):135–146
55 Cho JR, Lee CY, Lee J, et al. MicroRNA-761 inhibits Angiotensin II-induced vascular smooth muscle cell proliferation and migration by targeting mammalian target of rapamycin. Clin Hemorheol Microcirc 2015;63(01):45–56

